DOI: 10.1002/adma.200700609

# Spontaneous Chemical Vapor Growth of NiSi Nanowires and Their Metallic Properties**

By *Cheol-Joo Kim*, *Kibum Kang*, *Yun Sung Woo*, *Kyung-Guk Ryu*, *Heesung Moon*, *Jae-Myung Kim*, *Dong-Sik Zang*, and *Moon-Ho Jo**

One-dimensional metallic nanostructures offer challenging opportunities to investigate their possible applications as interconnects in electronic circuitry[1] and as field emitters in field emission displays.[2] In particular, metallic silicide nanowires are promising candidates, because their growth can be easily integrated with silicon processing technology.[3–5] Indeed the synthesis of single-crystalline, transition metal silicide nanowires, such as $TaSi_2$,[6] ε-FeSi,[7] and CoSi,[8] has been recently reported using diverse methods. The synthetic methods employed involve relatively high temperature processes,[6–8] and may not be compatible with the low temperature processes required for their practical applications into electronic and display devices. In contrast, single-crystalline Ni-silicide nanowires, which have been experimentally verified to possess intrinsically low resistivity at low dimensions compared with the others,[3] can be processed at relatively low temperatures, thus can provide practical advantages. For example, Wu et al.[3] reported highly metallic properties of single-crystalline NiSi nanowires fabricated by a solid-state reaction at 550 °C between individual Si nanowires and Ni overshells. Here a simpler and controlled synthesis at low temperatures (~400 °C) is reported, where single-crystalline NiSi nanowires spontaneously grow by $SiH_4$ chemical vapor deposition (CVD) on Ni thin films predeposited on various substrates, such as $SiO_2$/Si, quartz, and indium tin oxide (ITO) substrates. In fact, the Ni-catalyzed vapor phase thin film deposition has been previously investigated for applications into Si microelectronics and photovoltaics.[9,10] Specifically, the dimensionality of the Ni-silicides have been reproducibly directed from thin films to single-crystalline nanowires, as well as their phases, by fine-tuning of growth parameters during CVD of a $SiH_4$ gas precursor on predeposited Ni thin films. It is noted that Decker et al.[4] and Kim et al.[11–13] recently reported similar Ni-silicide nanowire growth by CVD and sputtering, however, the detailed growth mechanism, which is the main focus of this study, is unavailable to date. Here, by providing close observations of the morphological and phase evolution of Ni-silicide nanowires under optimized growth conditions, the spontaneous nanowire growth mechanism is discussed based on one-dimensional nucleation and growth of NiSi at a low supersaturation limit along with one-dimensional Ni diffusion during the chemical vapor reaction. Single-crystalline NiSi nanowires in this study exhibit typical metallic behaviors, and show promising field-emission properties. It is suggested that our simple method to spontaneously grow NiSi nanowires at low temperatures can provide a practical strategy to fabricate metallic nanostructures based on bottom-up synthetic approaches.

Our synthetic approach employs the Ni-catalyzed decomposition of $SiH_4$,[14] which can occur well below the thermal decomposition temperature of $SiH_4$ at above 600 °C. Thermally evaporated Ni thin films of 60–80 nm in thickness are used. During the CVD of $SiH_4$ within the wide range of precursor partial pressures and growth temperatures of 10–100 torr and 250–600 °C, the reaction produces either Ni-silicide thin films or nanowires of various phases. Figure 1 illustrates the evolution of the morphology and the phases of Ni-silicides, grown at 250, 400, and 600 °C at 50 torr of $SiH_4$, with the corresponding scanning electron microscopy (SEM) images, X-ray diffraction (XRD), and element depth profiling by Auger spectrometry. Within the entire growth range, Ni-silicide thin films have been commonly formed on the substrates; however, the surface morphology of the Ni-silicide thin films has been modified from planar sheets to nanowires, as well as phases in Ni-to-Si stoichiometry. The observations from Figure 1 are summarized in the following within the framework of $SiH_4$ vapor–Ni solid reactions, where $SiH_4$ decomposition and solid Ni diffusion are both thermally activated. First, at 250 °C, the catalyzed decomposition of $SiH_4$ and the Ni out-diffusion from the pre-deposited Ni thin films are not sufficient to turn the Ni film into a Ni-silicide thin film during the reaction, and

[*] Prof. M. H. Jo, C. J. Kim, K. Kang, Y. S. Woo, K. G. Ryu
Department of Materials Science and Engineering
Pohang University of Science and Technology (POSTECH)
San 31, Hyoja-Dong, Nam Gu, Pohang, Gyungbuk 790-784 (Korea)
E-mail: mhjo@postech.ac.kr
H. S. Moon, J. M. Kim, D. S. Zang
Samsung SDI Coporate R&D Center
428–5, Gongse-Ri, Geheung-Eup, Yongin-Si, Geonggi-Do 449-577 (Korea)

[**] This work was supported by the Nano R&D Program through the Korea Science and Engineering Foundation (2007-02864), the Korea Foundation for International Cooperation of Science & Technology, (KICOS) through a grant provided by the Korean Ministry of Science & Technology (MOST) in 2007 (No. K20716000006-07A0400-00610), the Korean Research Foundation Grant MOEHRD (KRF-2005-005-J13103), the "System IC 2010" project of the Korean Ministry of Commerce, Industry and Energy, and the POSTECH Core Research Program.

ADVANCED MATERIALS

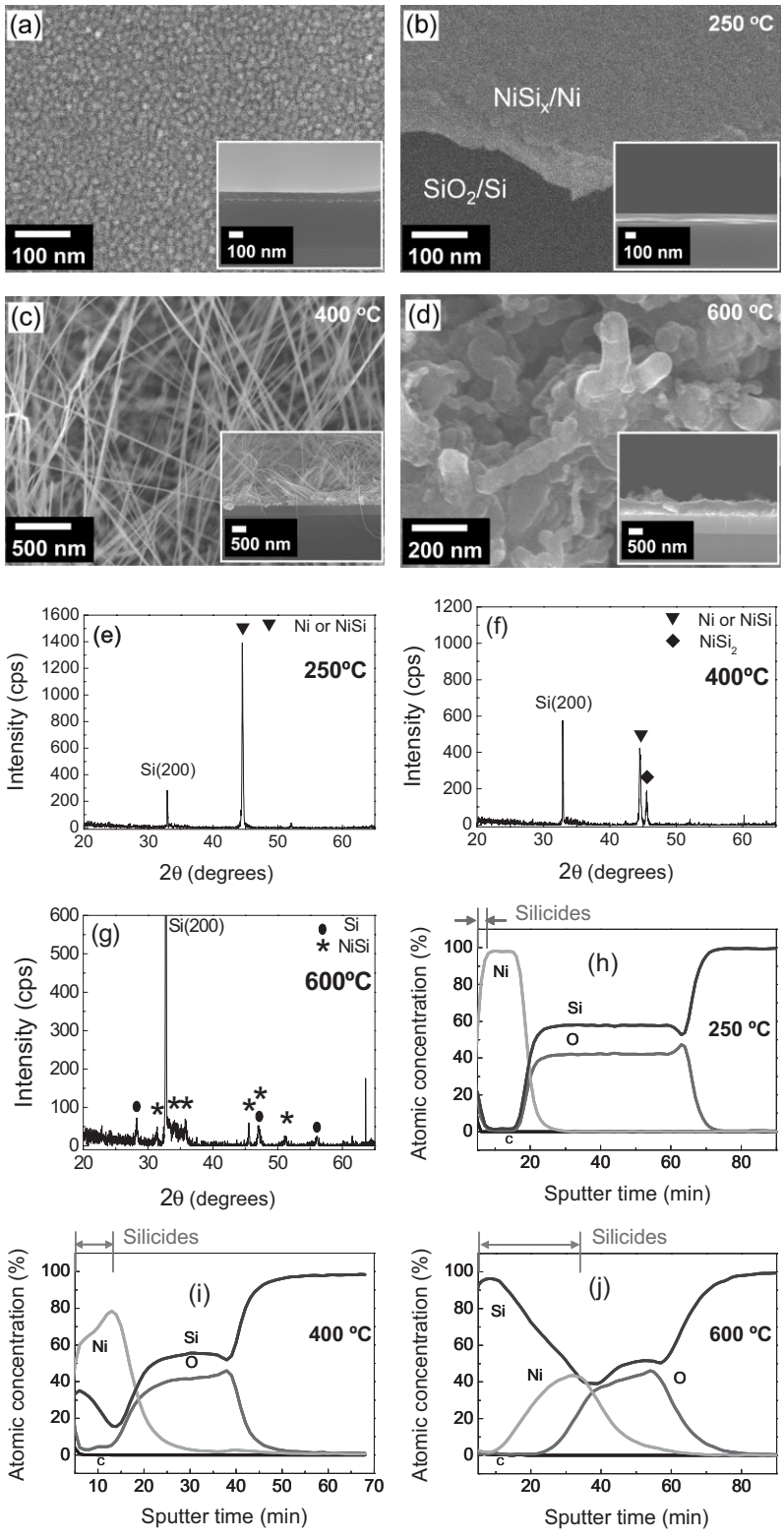


**Figure 1.** The evolution in the morphology and the phase of Ni-silicides grown at different temperatures on $SiO_2$/Si substrates. The first row shows plan-view and cross-sectional SEM images of: a) pre-deposited Ni films, b) Ni-silicide thin films grown at 250 °C, c) Ni-silicide nanowires grown at 400 °C, and d) Ni-silicide thin films grown at 600 °C. The corresponding XRDs and elemental profiles by Auger spectrometry of (b) (c) and (d) are in the second and third row, respectively. The plan-view of (b) is slightly tilted for clarity.

consequently it only forms a very thin NiSi overlayer on the Ni thin films. Meanwhile, at 600 °C, the decomposition of $SiH_4$ and Ni diffusion is sufficient or even excessive, and as a result the reaction forms 470 nm thick films of various Ni-silicide phases, which include both Ni-rich and Si-rich Ni-silicides. Lastly, Ni-silicide nanowires are formed at the surface during the reaction at around 400 °C, and they appear to be a NiSi phase on top of a Ni-rich phased film of 200 nm in thickness.

The spontaneous growth of Ni-silicide nanowires at 400 °C can be adapted to grow on other transparent substrates. Figures 2a–c show representative plan-view SEM images of Ni-silicide nanowires grown on $SiO_2$/Si, quartz, and ITO substrates, and essentially the same growth characteristics as seen in Figure 1 are observed, although the nanowire density is not optimized in each case. The synthesized nanowires typically range from 20 to 50 nm in diameter with a length of above 20 μm. Transmission electron microscopy (TEM) images of Figures 2d–f demonstrate that the nanowires are single-crystalline NiSi, i.e., the lattice spacing of 0.2 nm corresponds to that of (210) planes of NiSi, despite that the crystallographic orientation along the wire axis differs from nanowire to nanowire. The energy dispersive X-ray (EDX) spectra measured in various spots on individual nanowires (Fig. 2f) also confirms that the relative composition of Si and Ni is almost 1 : 1, i.e., they are NiSi nanowires.

Electrical resistivity of individual NiSi nanowires was measured by two-terminal configurations by applying direct current (DC) voltage from Ni/Au contacts across the individual nanowires, as representatively seen in the inset of Figure 3a. Figure 3a shows the typical current–voltage characteristics of a NiSi nanowire of 20 nm in diameter, from which the resistivity is calculated to be about 2.86 mΩ cm at 300 K. The maximum current that flows though this nanowire is 106 μA at 2.1 V, which corresponds to a current density of $3.4 \times 10^7$ A cm$^{-2}$. The measured resistivity is higher than the lowest value of 10 μΩ cm of NiSi thin films and nanowires measured with four-probe configurations, which can preclude contact resistance.[3,15,16] At the moment the relatively higher resistivity of the NiSi nanowires reported here are currently under investigation. Nevertheless, as in Figure 3b, the measured resistivity linearly decreases with decreasing temperature down to 77 K, as is typically expected for a metal. As for the practical application of the metallic proper-

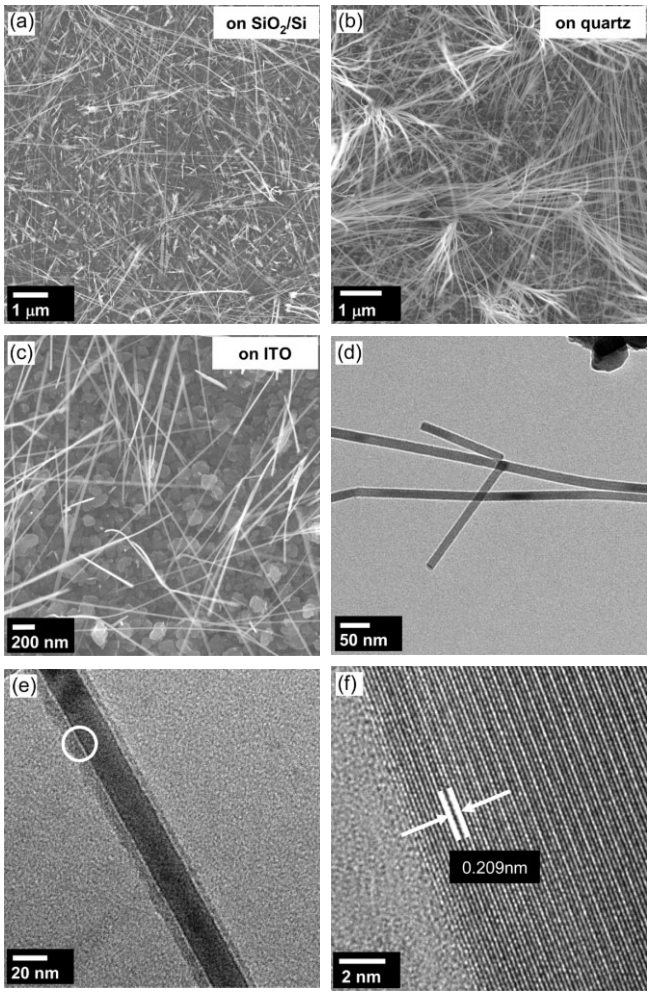


**Figure 2.** Plan-view SEM images of Ni-silicide nanowires grown on: a) $SiO_2$/Si substrates, b) quartz, and c) ITO substrates. TEM images of Ni-silicide nanowires at different magnifications in (d) (e) and (f) show the nanowires are single-crystalline NiSi.

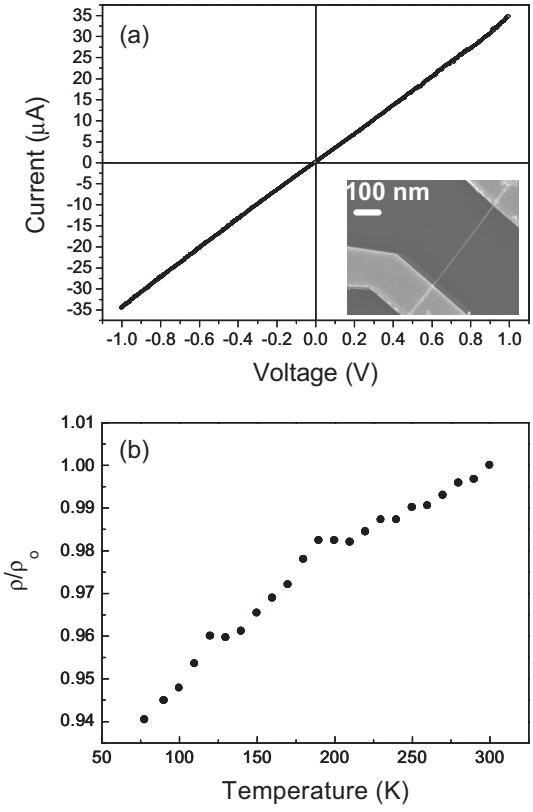


**Figure 3.** a) The current–voltage characteristics of an individual NiSi nanowire by two-probe configurations, as shown in the SEM image in the inset. b) The resistivity normalized with that measured at room 300 K as a function of temperature down to 77 K.

ties of the NiSi nanowires, they have been characterized for their field-emission properties based on square-shaped samples grown on $SiO_2$/Si and ITO substrates of $0.7 \times 0.7$ cm$^2$ in area in a vacuum of $1 \times 10^{-7}$ torr, as shown in the inset of Figure 4a. In both cases, the underlying Ni-silicide thin films were used as cathode contacts. Figure 4a shows the current density ($J$) versus the applied electrical field ($E$) between the anode and the cathode. The turn-on field for field-emission is defined as the value of the applied voltage to produce 10 μA cm$^{-2}$, and they all fall in the values below 3–4 V μm. Although the values reported here are higher than the lowest values reported for carbon nanotube strands, they are still lower than those recently reported for silicon[17] and other silicide nanowire emitters.[18,19] The quantitative degree of the local field enhancement from the emission tip geometry can be often assessed by the linear fit to the $\ln(J/E^2) - (1/E)$ relation based on the Fowler–Nordheim tunneling emission, expressed by $J = (A\beta E^2/\Phi)\exp(-B\Phi^{3/2}/\beta E)$, where β is the field enhancement factor, Φ is the work function of the emitter, and $A$ and $B$ are constants. The relation of $\ln(J/E^2) - (1/E)$ in the SiNi nanowire emitters, as in Figure 4b, is linearly fitted in the emission region with $\Phi = 4.7$ eV of NiSi, and the value of β is extracted to be 2200, which is higher than other nanowire emitters, such as Si nanowires,[17] $TaSi_2$ nanowires,[6] and oxide nanowires.[20,21]

A growth mechanism for the NiSi nanowires in the context of chemical vapor reactions based on the experimental observations of this study is presented. Specifically, the morphological evolution of the synthesized NiSi nanowires is discussed with respect to the role of Ni as a self-catalyst and a diffuser during the reaction, when the degree of supersaturation of Si vapor is closely controlled near the optimum nanowire synthesis conditions. Figures 5a–c show the morphological changes of the NiSi nanowires when the pressure is varied slightly near the optimum conditions of 50 torr of $SiH_4$ at a constant temperature of 400 °C. When the $SiH_4$ pressure increases from 50 to 75 and 100 torr, the nanowires are not clearly separated from one another and rather form a dendritic structure. As has been reported in several nanowire syntheses that employ vapor phase reactions, the relatively low supersaturation degree favours one-dimensional morphologies because of the limited nucleation sites, whereas the relatively higher supersaturation leads to a bulk morphology be-

  

ADVANCED MATERIALS

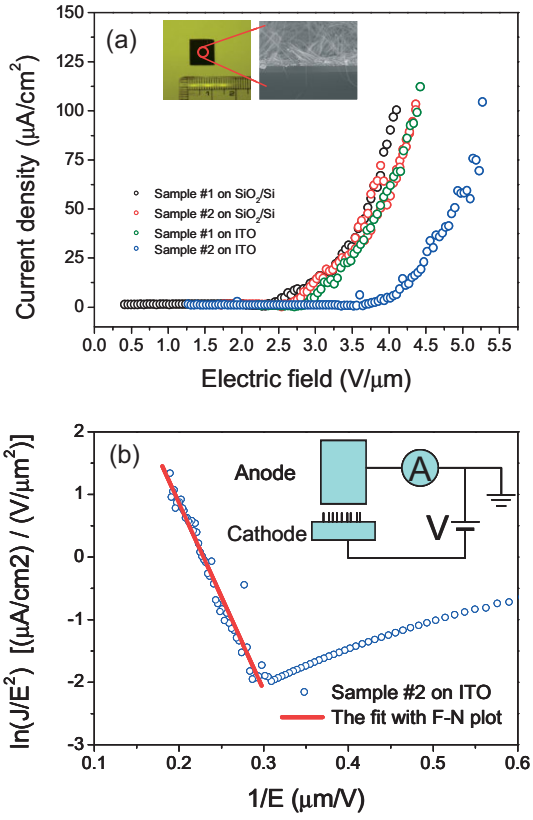


**Figure 4.** The field emission current versus the applied electrical field measured in a vacuum of $1 \times 10^{-7}$ torr from a Ni-silicide nanowire sample grown on $SiO_2$/Si and ITO substrates. The sample is square-shaped and $0.7 \times 0.7$ cm$^2$ in area, and the distance between the cathode and the anode is 450 μm.

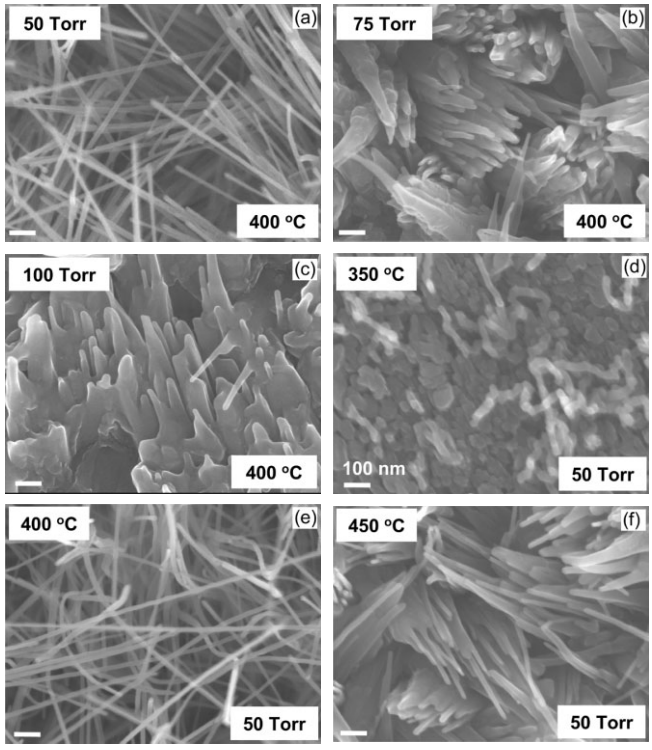


**Figure 5.** The morphological evolution of Ni-silicide nanowires near the optimum conditions, when the pressure varies from a) 50, b) 75, and c) 100 torr of $SiH_4$ at a constant temperature of 400 °C. A similar trend is observed for the growth temperature changes from d) 350, e) 400, and f) 450 °C at a constant pressure of 50 torr of $SiH_4$.

cause of homogeneous nucleation in the vapor phase.[22–25] Provided that the $SiH_4$ pressure is the measure of supersaturation of the gaseous Si phase during the reaction and the Ni diffusion is constant at a fixed temperature, the above observation can be understood with the prevailing role of supersaturation on the morphological determination. That is, the relatively low supersaturation at the low pressure favours the formation of a nanowire morphology as in Figure 5a, over the dendritic morphology at the relatively high supersaturation of high pressures as in Figures 5b and c. A similar morphological variation can be clearly observed in the sequence of Figures 5d–f, when the growth temperature increases from 350 to 400 and 450 °C. Short nanowires, scarcely formed on the rough surface of Ni-silicide thin films at 350 °C, increase their spatial density and length at 400 °C, and finally form a dendritic structure at 450 °C. Since Ni-catalyzed decomposition of $SiH_4$ is known to be thermally activated in this temperature range,[5] the structures observed in Figures 5d–f can be inferred from the fact that the higher temperature promotes the higher supersaturation, as discussed above.

In the solid-solid reactions of Ni and Si at the intermixing interface, it is generally accepted that the reaction is diffusion-limited and Ni is the faster diffuser.[5,26] Ni diffusion occurs through preformed silicide layers, thus the various silicide phases form sequentially starting from Ni-rich phases to Si-rich phases.[5,25] A similar observation has been made in the case of the Ni-catalyzed Si crystallization from Si vapor.[9] It is noted that this is also consistent with the observations of Figure 1, in which Ni-diffusion is thermally activated in the temperature range from 250 to 600 °C. Figure 6 shows the composition gradient in individual nanowires of Figure 5a, determined from the EDX spectra probed by the convergent electron beam along the entire nanowire, as also summarized in Table 1. It is observed that Ni is gradually depleted at the top end of the nanowires (marked as 'd' and 'e') over several hundreds of nanometers in length, whereas it is more accumulated at the bottom (marked as 'a' and 'b'), which is attached to the rumps over a similar length scale. The majority of the middle regions in the nanowire (marked as 'c') over several micrometers have a Ni-to-Si stoichiometry of approximately 1:1. The results suggest that Ni is supplied to the reaction front by one-dimensional diffusion across the several Ni-silicide phases within the nanowires as well as silicide thin films underneath, and catalytically reacts with the $SiH_4$ vapor to form Ni-silicides.

It is of particular interest to investigate the epitaxial and morphological relationship in the growth of NiSi nanowires on Ni-silicide thin films. Recent studies on the growth of silicide nanowires suggest that one-dimensional growth occurs

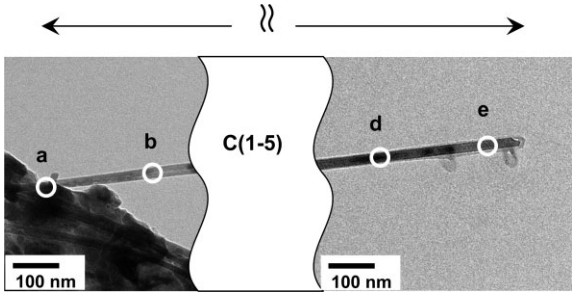


**Figure 6.** The composition gradient in individual nanowires of Figure 5d, determined from EDX spectra probed by the convergent electron beam along the entire nanowire. The middle region in a white shade that extends to 15 μm is not shown, because of the scale of the image.

**Table 1.** The relative compositions of Si and Ni at various positions within the individual nanowire. The values at region 'c' are averaged from five different positions, which are almost the same within the 5 % variation.

| Site | Elemental composition [at %] | |
|---|---|---|
| | Ni | Si |
| a | 61 | 39 |
| b | 44 | 56 |
| c (1–5) | 53 | 47 |
| d | 38 | 62 |
| e | 29 | 71 |

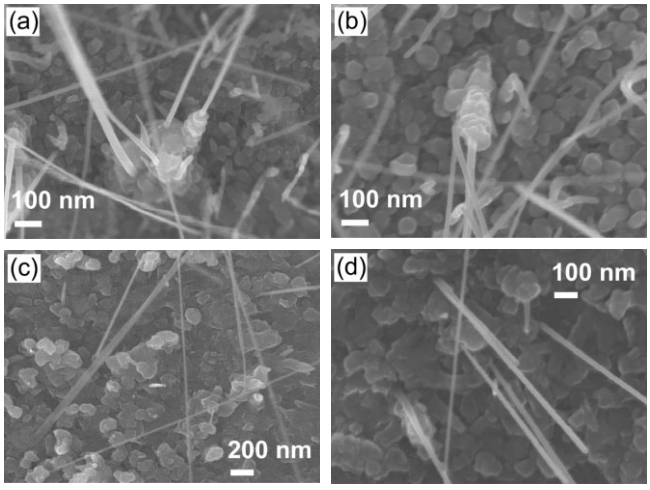


**Figure 7.** SEM images of the initial stages of Ni-silicide nanowires, where the nanowires grow out from either the top of islands or the valley of islands of thin films.

on the top of islands because of thermodynamic energy minimization.[4,6,11–13] It has also been long suggested that the one-dimensional growth proceeds by axial screw dislocation[27] during the vapour condensation. In this study, however, a unified morphological relationship during the initial stages of nanowire growth has not been observed, as typically shown in Figure 7, where NiSi nanowires grow out from either the top or the valley of islands. The exact relation between the microscopic surface morphology and the one-dimensional nucleation/growth requires further investigation.

In summary, a simple chemical vapor growth of single-crystalline NiSi nanowires at 400 °C is demonstrated. One-dimensional growth of NiSi in our study can be understood based on the combination of the control of supersaturation of $SiH_4$ and Ni diffusion, which are both thermally activated. Specifically, observations of the nanowire growth are discussed based on limited nucleation at low supersaturation degree during the reaction and one-dimensional Ni diffusion. The NiSi nanowires synthesized here exhibit typical metallic properties and promising field-emission properties. The simple and low temperature synthesis of single-crystalline NiSi nanowires in this study can provide interesting strategies to fabricate metallic nanostructures for their possible applications as interconnects in Si microelectronics and field emitters in field emission displays.

It is noted that during the submission of this Communication, Song et al. reported a synthesis of $Ni_2Si$ nanowires by vapor transport using $Ni_2Si$ powders.[28]

## *Experimental*

Single-crystalline NiSi nanowires were synthesized by CVD using a $SiH_4$ gas precursor on pre-deposited Ni films. Ni thin films were prepared by thermal evaporation of Ni with a nominal thickness of 60–80 nm on $SiO_2$/Si (100) substrates, as well as quartz and ITO substrates at room temperature. Hot-wall CVD growth was carried out in a quartz tube under a 50 sccm flow of $SiH_4$ (specifically, 10 % $SiH_4$ premixed in $H_2$) for 15 min at various temperatures. The effects of the growth temperature and the $SiH_4$ partial pressure on the optimum growth of NiSi nanowires was investigated, where they varied from 250 to 600 °C and 10 to 100 torr, respectively. The Ni-silicide nanowires were characterized by SEM for their morphology, and by TEM and EDX for their crystallinity and composition. Two-terminal electrical transport measurements were performed on individual NiSi nanowires under vacuum at various temperatures, where electrical contacts were defined by e-beam lithography and the Ni/Au (30/100 nm) lift-off. The electron field-emission from the NiSi nanowires was measured using as-grown, square-shaped samples of $0.7 \times 0.7$ cm$^2$ in a vacuum of $1 \times 10^{-7}$ torr by applying a DC voltage across the distance of 450 μm between the anode and the cathode.

Received: March 13, 2007
Revised: May 22, 2007
Published online: October 16, 2007

[1] J. Li, Q. Ye, A. Cassell, H. T. Ng, R. Stevens, J. Han, M. Meyyappan, *Appl. Phys. Lett.* **2003**, *82*, 2491.
[2] L. Gangloff, E. Minoux, K. B. K. Teo, P. Vincent, V. T. Semet, V. T. Binh, M. H. Yang, I. Y. Y. Bu, R. G. Lacerda, G. Pirio, J. P. Schnell, D. Pribat, D. G. Hasko, G. A. J. Amaratunga, W. I. Milne, P. Legagneux, *Nano Lett.* **2004**, *4*, 1575.
[3] Y. Wu, J. Xiang, C. Yang, W. Lu, C. M. Lieber, *Nature* **2004**, *430*, 61.
[4] C. A. Decker, R. Solanki, J. L. Freeouf, J. R. Carruthers, D. R. Evans, *Appl. Phys. Lett.* **2004**, *84*, 1389.
[5] J. P. Gambino, E. G. Colgan, *Mater. Chem. Phys.* **1998**, *52*, 99.
[6] Y. L. Chueh, M. T. Ko, L. J. Chou, L. J. Chen, C. S. Wu, C. D. Chen, *Nano Lett.* **2006**, *6*, 1637.

  

ADVANCED MATERIALS


[7] O. Y. Lian, E. S. Thrall, M. M. Deshmukh, H. Park, *Adv. Mater.* **2006**, *18*, 1437.

[8] a) A. L. Schmitt, L. Zhu, D. Schmeisser, F. J. Himpsel, S. Jin, *J. Phys. Chem. B* **2006**, *110*, 18142. b) A. L. Schmitt, M. J. Bierman, D. Schmeisser, F. J. Himpsel, S. Jin, *Nano Lett.* **2006**, *6*, 1617.

[9] E. A. Guliants, W. A. Anderson, L. P. Guo, V. V. Guliants, *Thin Solid Films* **2001**, *385*, 74.

[10] C. Lavoie, F. M. d'Heurle, C. Detavernier, C. Cabral Jr., *Microelectron. Eng.* **2003**, *70*, 144.

[11] J. Kim, W. A. Anderson, Y. J. Song, G. B. Kim, *Appl. Phys. Lett.* **2005**, *86*, 253101.

[12] J. Kim, W. A. Anderson, *Thin Solid Films* **2005**, *483*, 60.

[13] J. Kim, W. A. Anderson, *Nano Lett.* **2006**, *6*, 1356.

[14] L. H. Dubois, R. G. Nuzzo, *J. Vac. Sci. Technol., A* **1984**, *2*, 441.

[15] J. Eberhardt, E. Kasper, *Semicond. Sci. Technol.* **2001**, *16*, L47.

[16] G. Ottaviani, *J. Vac. Sci. Technol.* **1979**, *16*, 1112.

[17] Y. L. Chueh, L. J. Chou, S. L. Cheng, J. H. He, W. W. We, L. J. Chen, *Appl. Phys. Lett.* **2005**, *86*, 133112.

[18] Y. W. Ok, T. Y. Seong, C. J. Choi, K. N. Tu, *Appl. Phys. Lett.* **2006**, *88*, 043106.

[19] Q. Xiang, Q. X. Wang, Z. Wang, X. Z. Zhang, L. Q. Liu, J. Xu, D. P. Yu, *Appl. Phys. Lett.* **2005**, *86*, 243103.

[20] Y. K. Tseng, C. J. Huang, H. M. Cheng, I. N. Kin, K. S. Liu, I. C. Chen, *Adv. Funct. Mater.* **2003**, *87*, 73109.

[21] J. H. He, T. H. Wu, C. L. Hsin, K. M. Li, L. J. Chen, Y. L. Chueh, L. L. J. Chou, Z. L. Wang, *Small* **2006**, *2*, 116.

[22] Y. Xia, P. Yang, Y. Sun, Y. Wu, B. Mayers, B. Gates, Y. Yin, F. Kim, H. Yan, *Adv. Mater.* **2003**, *15*, 353.

[23] B. S. Guiton, Q. Gu, A. L. Prieto, M. S. Gudiksen, H. Park, *J. Am. Chem. Soc.* **2004**, *127*, 498.

[24] Z. W. Pan, Z. R. Dai, Z. L. Wang, *Science* **2001**, *291*, 1947.

[25] G. W. Sears, *Acta Metall.* **1955**, *3*, 367.

[26] F. M. d'Heurle, P. Gas, *J. Mater. Res.* **1986**, *1*, 205.

[27] S. S. Brener, G. W. Sears, *Acta Metall.* **1955**, *4*, 268.

[28] Y. Song, A. L. Schimitt, S. Jin, *Nano Lett.* **2007**, *7*, 965.